*Inorg. Chem.* **2004**, *43*, 6093–6100

# Mechanistic Elucidation of the Substitution Behavior of Alkyl Cobaloximes in Water and Methanol as Solvents

**Basam M. Alzoubi, GUnter Liehr, and Rudi van Eldik***

*Institute for Inorganic Chemistry, University of Erlangen−Nürnberg, Egerlandstr. 1, 91058 Erlangen, Germany*

Received February 23, 2004

The ligand substitution behavior of *trans*-[Co(Hdmg)$_2$(R)S] (R = $CH_3$, $PhCH_2$; Hdmg = dimethylglyoximate; S = $H_2O$ and/or MeOH) was studied for imidazole, pyrazole, 1,2,4-triazole, *N*-acetylimidazole, 5-chloro-1-methylimidazole, $NO_2^-$, $Ph_3P$, $Ph_3As$, and $Ph_3Sb$ as entering ligands. In all cases, except for $Ph_3As$ and $Ph_3Sb$, the observed kinetics shows a linear dependence on the entering nucleophile concentration with no evidence for a back reaction. In the case of $Ph_3As$ and $Ph_3Sb$ as entering nucleophiles, kinetic evidence for a reverse solvolysis reaction is at hand. Activation parameters ($\Delta H^{\ddagger}$, $\Delta S^{\ddagger}$, and $\Delta V^{\ddagger}$) were determined from the temperature and pressure dependence of all studied reactions and support the operation of a dissociatively activated substitution mechanism. The rate and activation parameters show that there is an increase in the dissociative character from a dissociative interchange to a limiting dissociative mechanism that depends on the nature of R and the entering nucleophile. The crystal structure of *trans*-[Co(en)$_2$(Me)$H_2O$]$^{2+}$ was determined by X-ray analysis. The Co–O and Co–C bond lengths were found to be 2.153(6) and 1.995(10) Å, respectively. The kinetic and structural data are discussed in reference to a series of earlier studied systems for which data are reported in the literature.

## Introduction

Over the past few years, we have developed an active interest in the systematic tuning of the substitution behavior of alkylcobalt(III) complexes for various reasons. First of all, such reactions are relevant to the mechanistic behavior of coenzyme $B_{12}$, a bio-organometallic cofactor with a cobalt−carbon bond. Second, the introduction of a single cobalt−carbon bond in Co(III) complexes has a profound influence on their substitution lability. Third, such complexes allow a systematic adjustment of their reactivity via steric hindrance and electron donor/acceptor effects of spectator ligands and the coordinated alkyl or aryl group. Such studies are of fundamental interest in the elucidation of inorganic/bioinorganic reaction mechanisms and serve as model systems for tuning the lability of inert metal complexes.

In this respect, it is interesting to note that many investigations in the past have focused on the mechanistic behavior of coenzyme $B_{12}$ itself, or on modified forms of the coenzyme, or on closely related model systems with a quite different chelate arrangement around the Co(III) center. By way of comparison, the substitution behavior of vitamin $B_{12}$ derivatives, especially aquacobalamin, was investigated as a reference system in which the cobalt−carbon bond is substituted by a cobalt−water bond that has no labilization effect on the Co(III) center. Work in our laboratories has focused on the substitution behavior of coenzyme $B_{12}$ and modified alkylcobalamins with R = Et, Pr, Me, $CF_3CH_2$, $NCCH_2$, $CF_3$, and CN,[1] *trans*-[Co(en)$_2$(Me)$H_2O$]$^{2+}$,[2] *trans*-[Co(en)$_2$(Me)$NH_3$]$^{2+}$,[2b] *trans*-[Co(BQDI)$_2$($PPh_3$)S]$^+$ (BQDI = *o*-benzosemiquinonediimine; S = MeOH, MeCN),[3] [Co(LNHPy)(HLNHPy)(R)]$^+$ (HLNHPy = 2-(2-pyridylethyl)-amino-3-butanone oxime; R = Et, Me, $CF_3CH_2$, bridging-$CH_2$),[4] and *trans*-[Co(Hdmg)$_2$(R)S] (Hdmg = dimethylglyoximate; R = *cyclo*-$C_5H_9$, Et, Me, Ph, $PhCH_2$, $CF_3CH_2$; S = $H_2O$, MeOH).[5,6] In these studies, detailed kinetic inves-

* To whom correspondence should be addressed. E-mail: vaneldik@chemie.uni-erlangen.de.

(1) Hamza, M. S. A.; van Eldik, R. *Dalton Trans*. **2004**, 1.
(2) (a) Hamza, M. S. A.; Dücker-Benfer, C.; van Eldik, R. *Inorg. Chem*. **2000**, *39*, 3777. (b) Alzoubi, B. M.; Hamza, M. S. A.; Dücker-Benfer, C.; van Eldik, R. *Eur. J. Inorg. Chem*. **2002**, 968.
(3) Alzoubi, B. M.; Hamza, M. S. A.; Dücker-Benfer, C.; van Eldik, R. *Eur. J. Inorg. Chem*. **2003**, 2972.
(4) Alzoubi, B. M.; Hamza, M. S. A.; Felluga, A.; Randaccio, L.; Tauzher, G.; van Eldik, R. *Eur. J. Inorg. Chem*. **2003**, 3738.
(5) Hamza, M. S. A.; Felluga, A.; Randaccio, L.; Tauzher, G.; van Eldik, R. *Dalton Trans*. **2004**, 287.
(6) Alzoubi, B. M.; Hamza, M. S. A.; Felluga, A.; Randaccio, L.; Tauzher, G.; van Eldik, R. *Eur. J. Inorg. Chem*. **2004**, 653.

10.1021/ic049761j CCC: $27.50 
Published on Web 08/21/2004

tigations enabled the determination of rate and activation parameters, on which basis detailed mechanistic assignments could be made. For instance, for the reaction of cyanide with different alkylcobalamins it was found that the nature of the alkyl group has a marked influence on the thermodynamic stability constants and the kinetics and mechanism of the substitution reactions of the axial ligand *trans* to the alkyl group.[1,7,8]

The Co−C bond length depends on three contributing factors. First, there are *cis* steric interactions, distortions in the corrin macrocycle or equatorial ligand toward the axial *trans* alkyl ligand resulting in Co−alkyl bond lengthening. Second, a *trans* steric influence occurs when the bulkiness of an axial ligand induces an elongation or weakening of the *trans* metal−ligand bond. Third, the *trans* electronic influence is associated with how the change in basicity of the axial ligand affects the Co−alkyl bond length and/or bond dissociation energy (*trans* effect) and how changes in the $\sigma$-donor character of the alkyl group affect the Co−N(ax) bond distance.[9]

It is well-known that high-pressure techniques can assist the elucidation of inorganic and bioinorganic reaction mechanisms through the determination of activation volumes obtained from the pressure dependence of the rate constant and the construction of reaction volume profiles.[10,11] In the case of Co(III) complexes, activation volume data for complex-formation reactions of *trans*-$[Co(en)_2(Me)H_2O]^{2+}$ with $CN^-$, imidazole,[2a] and $NH_3$[2b] are similar to data for the reactions of aquacobalamin with different ligands such as *N*-acetylimidazole,[12] $HN_3$, $N_3^-$, pyridine and its derivatives, and thiourea and its derivatives.[13−15] In all these cases, $\Delta V^{\ddagger}$ was found to be in the range between +4 and +10 $cm^3$ $mol^{-1}$, an indication that the reactions follow an $I_d$ mechanism. These values are significantly smaller than those reported for substitution reactions of cobalt(III) porphyrin systems, where it was found that $\Delta V^{\ddagger}$ values for ligand substitution on $[Co(TMPP)(H_2O)_2]^{5+}$ and $[Co(TPPS)(H_2O)_2]^{3-}$, TMPP = *meso*-tetrakis(4-*N*-methylpyridyl)porphine and TPPS = *meso*-tetrakis(p-sulfonatophenyl)porphine, are +14.4 and +15.4 $cm^3$ $mol^{-1}$, respectively, and these were accordingly assigned to a limiting D mechanism.[16,17]

In the present study, we have extended the work on *trans*-$[Co(Hdmg)_2(R)S]$ to R = Me and $PhCH_2$ (S = $H_2O$ and/or MeOH) and to a wide range of different entering nucleophiles (viz. imidazole, pyrazole, 1,2,4-triazole, *N*-acetylimidazole, 5-chloro-1-methylimidazole, $NO_2^-$, $Ph_3P$, $Ph_3As$, and $Ph_3Sb$) in order to determine the role of the nucleophilicity of the entering ligand and the nature of R on the reactivity of the Co(III) center. These data allow us to present an overall comparison of steric and electronic effects that control the reactivity of alkyl and aryl Co(III) complexes, in reference to a series of earlier studied systems for which data are reported in the literature.

## Experimental Section

**Materials.** All chemicals were of p.a. grade and used as received. Imidazole, pyrazole, 1,2,4-triazole, *N*-acetylimidazole, and methylhydrazine were purchased from Fluka, 5-chloro-1-methylimidazole from Acros, TAPS buffer from Sigma, and $Ph_3Sb$ from Strem. Triphenylphosphine, cobalt(II) nitrate hexahydrate, and sodium nitrite were purchased from Merck, and $Ph_3As$ from Aldrich. Ultrapure water was used in the kinetic measurements. *trans*-$[Co(Hdmg)_2(R)H_2O]$ (R = $CH_3$, $PhCH_2$) and *trans*-$[Co(en)_2(Me)H_2O]S_2O_6$ were prepared as previously reported and were characterized by elemental analysis and UV−vis and NMR spectroscopy; the results were in agreement with literature data.[18,19] Preparation of solutions and all measurements were carried out in the dark because the investigated complexes are light sensitive.

All the reactions in aqueous solution were studied at pH 9.0 by using TAPS buffer. The pH of 9.0 was selected to prevent protonation of the nitrogen donor nucleophiles and formation of the corresponding hydroxo complexes.

**X-ray Structure Determination.** Intensity data were collected on a Nonius CAD4 Mach3 diffractometer with graphite monochromated Mo K$\alpha$ radiation in the $\omega/2\theta$ scan mode at room temperature. The structure of *trans*-$[Co(en)_2(Me)H_2O]S_2O_6$ was solved by direct methods using SIR-97[20] and refined by full-matrix least-squares on $F^2$ using SHELXL-97.[21] Complete crystallographic details, bond lengths, bond angles anisotropic temperature factors, and hydrogen atom coordinates are available as a CIF file as Supporting Information. Some crucial bond lengths and bond angles are summarized in Table 1.

Crystal data: $CoC_5H_{21}N_4S_2O_7$, fw = 372.3 g $mol^{-1}$, $a$ = 19.913(10) Å, $b$ = 12.094(10) Å, $c$ = 11.754(10) Å, $\alpha = \beta = \gamma = 90°$, $V$ = 2831(4) $Å^3$, orthorhombic, space group = *Iba*2 (No. 45), $Z$ = 8, $D_c$ = 1.738 g $cm^{-3}$, $\mu$(Mo K$\alpha$) = 1.5 $mm^{-1}$, $T$ = 298 K, R1 = 0.066 for the data $F_o > 2\sigma(F_o)$, [22] ($R_{int}$ = 0.050 for 2335 unique reflections). The minimum and maximum electron densities on the final difference Fourier map were −0.51 and 0.89 e $Å^{-3}$, respectively.

**Instrumentation.** The pH of the solution was measured using a Mettler Delta 350 pH meter. The pH meter was calibrated with


(7) Hamza, M. S. A.; Zou, X.; Brown, K. L.; van Eldik, R. *Inorg. Chem.*, **2001**, *40*, 5440.
(8) Hamza, M. S. A.; Zou, X.; Brown, K. L.; van Eldik, R. *J. Chem. Soc., Dalton Trans*. **2002**, 3832.
(9) Hansen, L. M.; Kumar, P. N. V. P.; Marynick, D. S. *Inorg. Chem*. **1994**, *33*, 728.
(10) (a) *Inorganic High-Pressure Chemistry. Kinetics and mechanisms*; van Eldik, R., Ed.; Elsevier Biomedical: Amsterdam, Netherlands, 1986. (b) Drljaca, A.; Hubbard, C. D.; van Eldik, R.; Asano, T.; Basilevsky, M. V.; le Noble, W. J. *Chem. Rev*. **1998**, *98*, 2167. (c) *High-Pressure Chemistry: Synthetic, Mechanistic, and Supercritical Applications*; van Eldik, R.; Klärner, F.-G., Eds.; Wiley-VCH: Weinheim, Germany, 2002.
(11) (a) De Vito, D.; Weber, J.; Merbach, A. E. *Inorg. Chem*. **2004**, *43*, 858. (b) Grundler, P. V.; Salignac, B.; Cayemittes, S.; Alberto, R.; Merbach, A. E. *Inorg. Chem*, **2004**, *43*, 865.
(12) Hamza, M. S. A. *J. Chem. Soc., Dalton Trans*., **2002**, 2831.
(13) Meier, M.; van Eldik, R. *Inorg. Chem*. **1993**, *32*, 2635.
(14) Prinsloo, F. F.; Meier, M.; van Eldik, R. *Inorg. Chem*. **1994**, *33*, 900.
(15) Prinsloo, F. F.; Breet, E. L. J.; van Eldik, R. *J. Chem. Soc., Dalton Trans*. **1995**, 685.
(16) Funahashi, S.; Inamo, M.; Ishihara, K.; Tanaka, M. *Inorg. Chem.* **1982**, *21*, 447.
(17) Leipoldt, J. G.; van Eldik, R.; Kelm, H. *Inorg. Chem.* **1983**, *22*, 4146.
(18) Schrauzer, G. N.; Windgassen, R. J. *J. Am. Chem. Soc*. **1966**, *88*, 3738.
(19) Kofod, P.; Harris, P.; Larsen, S. *Inorg. Chem*. **1997**, *36*, 2258.
(20) Altomare, A.; Cascarano, G.; Giacovazzo, C.; Guagliardi, A.; Burla, M. C.; Polidori, G.; Camalli, M. SIR-92-Program Package for Solving Crystal Structures by Direct Methods. *J. Appl. Crystallogr*. **1994**, *27*, 435.
(21) Sheldrick, G. M. *SHELXL-97*; University of Göttingen: Göttingen, Germany, 1997. (a) Sheldrick, G. M. *Acta Crystallogr., Sect. A* **1990**, *A46*, 467−473. (b) Sheldrick, G. M. *Acta Crystallogr., Sect. D* **1993**, *D49*, 18−23. (c) Sheldrick, G. M.; Schneider, T. R. *Methods Enzymol*. **1997**, *227*, 319−343.
(22) $R1 = \sum(F_o - F_c)/\sum F_o$; $wR2 = [(\sum w(F_o^2 - F_c^2)^2/\sum w(F_o^2)^2]^{1/2}$.

**Table 1.** Bond Lengths (Å) and Bond Angles (deg) with Standard Deviations for the Complex *trans*-$[Co(en)_2(Me)H_2O]S_2O_6$

| bond distance (Å) | | bond angle (deg) | |
|---|---|---|---|
| Co−O1 | 2.153(6) | O1−Co−N1 | 88.2(3) |
| Co−N1 | 1.999(7) | O1−Co−N2 | 89.5(3) |
| Co−N2 | 1.995(8) | O1−Co−N3 | 90.2(3) |
| Co−N3 | 1.931(7) | O1−Co−N4 | 87.8(3) |
| Co−N4 | 1.927(7) | O1−Co−C5 | 177.6(3) |
| Co−C5 | 1.995(10) | N1−Co−N2 | 84.2(3) |
| N1−C1 | 1.453(12) | N1−Co−N3 | 176.3(3) |
| N2−C2 | 1.437(12) | N1−Co−N4 | 96.0(3) |
| N3−C3 | 1.553(11) | N1−Co−C5 | 89.4(3) |
| N4−C4 | 1.480(12) | N2−Co−N3 | 92.5(3) |
| C1−C2 | 1.512(14) | N2−Co−N4 | 177.2(3) |
| | | N2−Co−C5 | 90.6(4) |
| | | N3−Co−N4 | 87.3(3) |
| | | N3−Co−C5 | 92.2(3) |
| | | N4−Co−C5 | 92.1(3) |
| | | Co−N1−C1 | 108.4(5) |
| | | Co−N2−C2 | 109.1(6) |

standard buffer solutions at pH 4.0, 7.0 and 10.0. UV−vis spectra were recorded on Shimadzu UV-2101 and Hewlett-Packard 8452A spectrophotometers.

Kinetic measurements were carried out on an Applied Photophysics SX 18MV stopped-flow instrument coupled to an online data acquisition system. At least eight kinetic runs were recorded under all conditions, and the reported rate constants represent the mean values. All kinetic measurements were carried out under pseudo-first-order conditions; i.e., the ligand concentration was in at least a 10-fold excess. Measurements at high pressure were carried out using a homemade high-pressure stopped-flow unit.[23] Kinetic data were analyzed with the OLIS KINFIT program. All instruments used were thermostated to the desired temperature (±0.1 °C).

## Results and Discussion

The kinetics of the ligand substitution reactions (eq 1) of *trans*-$[Co(Hdmg)_2(R)S]$ (R = $CH_3$, $CH_2Ph$; S = $H_2O$, MeOH) were studied for different nucleophiles L to form *trans*-$[Co(Hdmg)_2(R)L]$. The UV−vis absorption spectra of *trans*-$[Co(Hdmg)_2(R)S]$ and *trans*-$[Co(Hdmg)_2(R)L]$ complexes, where L = imidazole, pyrazole, 1,2,4-triazole, *N*-acetylimidazole, 5-chloro-1-methylimidazole, $NO_2^-$, $Ph_3P$, $Ph_3As$, and $Ph_3Sb$, are summarized in Table 2.

$$\textit{trans}\text{-}[Co(Hdmg)_2(R)S] + L \underset{k_b}{\overset{k_a}{\rightleftharpoons}} \textit{trans}\text{-}[Co(Hdmg)_2(R)L]^{0/-} + S \quad (1)$$

Figures 1−3 and S1 (Supporting Information) report plots of the pseudo-first-order rate constant $k_{obs}$ versus [L] for the reactions with imidazole, pyrazole, 1,2,4-triazole, *N*-acetylimidazole, 5-chloro-1-methylimidazole, $NO_2^-$, and $Ph_3P$ at 25 °C. The linear plots have negligible intercepts, indicating that a reverse or parallel reaction does not contribute significantly under the selected experimental conditions. This behavior can be expressed by the rate law given in (eq 2) with a negligible contribution from $k_b$. The second-order rate constants for substitution of the solvent ($k_a$) were found to be 70.3, 90.7, 70.6, 48.2, 105.1, and 113.9 $M^{-1}$ $s^{-1}$ for L = imidazole, pyrazole, 1,2,4-triazole, *N*-acetylimidazole, 5-chloro-1-methylimidazole, and $NO_2^-$, respectively (R = $CH_3$, S = $H_2O$); 23.6 and 19.6 $M^{-1}$ $s^{-1}$ for L = imidazole and $Ph_3P$, respectively (R = $CH_3$, S = MeOH); and 252 $M^{-1}$ $s^{-1}$ for L = $Ph_3P$ (R = $PhCH_2$ and S = MeOH) at 25 °C.

$$k_{obs} = k_a[L] + k_b \quad (2)$$

Kinetic data for the reaction of *trans*-$[Co(Hdmg)_2(R)$-MeOH] with $Ph_3As$ and $Ph_3Sb$ are reported in Figures 4 and 5, from which it follows that good linear plots with significant intercepts are obtained within the experimental error limits. This behavior can also be expressed by the rate law given in eq 2, where $k_a$ and $k_b$ represent the rate constants

**Table 2.** UV−Vis Spectral Data for *trans*-$[Co(Hdmg)_2(R)(L)]$ in $H_2O$ and MeOH at Room Temperature

| L | $\lambda$, nm ($10^{-3}\epsilon$, $M^{-1}$ $cm^{-1}$) | $\lambda$ [f] (nm) |
|---|---|---|
| $H_2O$[b] | $278^{sh}$ [a] (4.94), 384 (1.43), and 440 (1.22) | |
| imidazole[b] | 282 (5.48), 372 (2.14), and $416^{sh}$ (0.85) | 450 |
| pyrazole[b] | 280 (5.84), 374 (1.91), and $420^{sh}$ (0.87) | 450 |
| 1,2,4-triazole[b] | 282 (5.74), 372 (2.11), and $416^{sh}$ (0.78) | 450 |
| *N*-acetylimidazole[b] | 372 (2.19) and $420^{sh}$ (0.82) | 450 |
| 5-chloro-1-methylimidazole[b] | 358 (3.37) and $414^{sh}$ (1.06) | 450 |
| $NO_2^-$ [b] | $422^{sh}$(1.04) and $464^{sh}$ (0.25) | 445 |
| MeOH[c] | $284^{sh}$ (6.45), 384 (1.70), and 444 (1.64) | |
| $Ph_3P$[c] | $370^{sh}$ (4.15) and $420^{sh}$ (1.23) | 445 |
| imidazole[c] | 288 (7.08), 372 (2.68), and $420^{sh}$ (0.93) | 445 |
| $Ph_3As$[c,d] | $308^{sh}$, $378^{sh}$, and 444 | 332 |
| $Ph_3Sb$[c,d] | $316^{sh}$, $372^{sh}$, and 448 | 335 |
| MeOH[e] | $274^{sh}$ (12.95), 358 (6.64), and 470 (1.06) | |
| $Ph_3P$[e] | $360^{sh}$ (14.43) | 410 |

[a] sh = shoulder. [b] *trans*-$[Co(Hdmg)_2(Me)(L)]$ in $H_2O$ (pH 9.0, $I$ = 0.1 M $NaClO_4$ and 0.5 M for $NO_2^-$ as nucleophile). [c] *trans*-$[Co(Hdmg)_2(Me)(L)]$ in MeOH. [d] No extinction coefficients are specified since only partial formation of the corresponding complex could be reached due to the unfavorable equilibrium position (see ratio of rate constants for the forward and reverse reactions given in Table 3). [e] *trans*-$[Co(Hdmg)_2(PhCH_2)(L)]$ in MeOH. [f] Wavelength at which kinetic data were recorded.

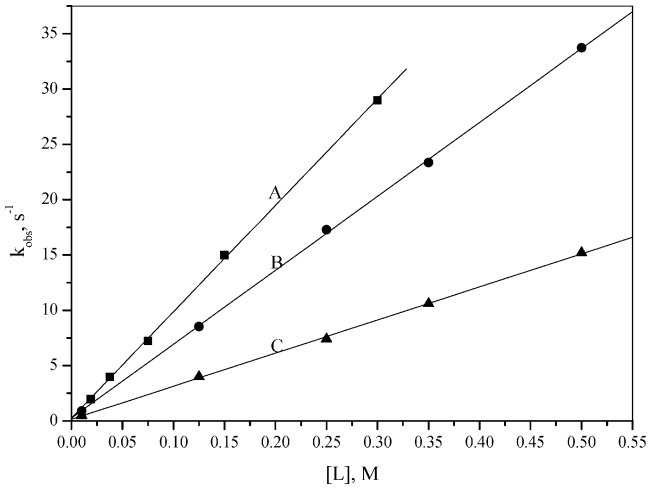


**Figure 1.** Plots of $k_{obs}$ versus [5-chloro-methylimidazole] (A), [pyrazole] (B), and [*N*-acetylimidazole] (C) for the reaction with $1 \times 10^{-4}$ M *trans*-$[Co(Hdmg)_2(Me)H_2O]$ at 25.0 °C, pH 9.0, and $I$ = 0.1 M $NaClO_4$.

(23) van Eldik, R.; Gaede, W.; Wieland, S.; Kraft, J.; Spitzer, M.; Palmer, D. A. *Rev. Sci. Instrum.* **1993**, *64*, 1355.

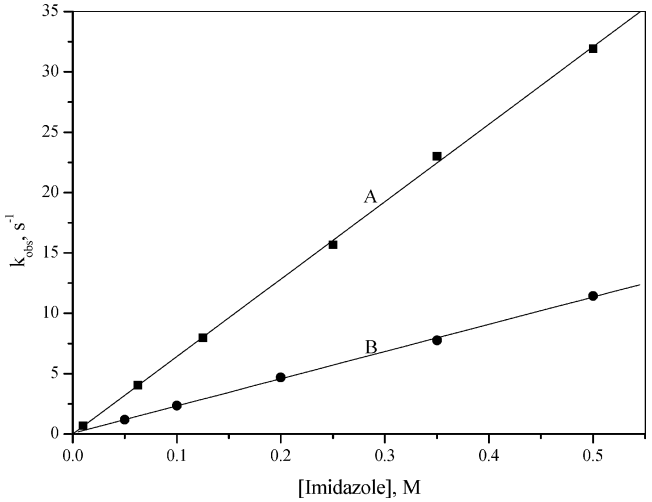


**Figure 2.** Plots of $k_{obs}$ versus [imidazole] for the reaction with $1 \times 10^{-4}$ M *trans*-[Co(Hdmg)$_2$(Me)S] where S = $H_2O$ (A) and MeOH (B) at 25.0 °C, pH 9.0, and $I = 0.1$ M $NaClO_4$ for aqueous solution.

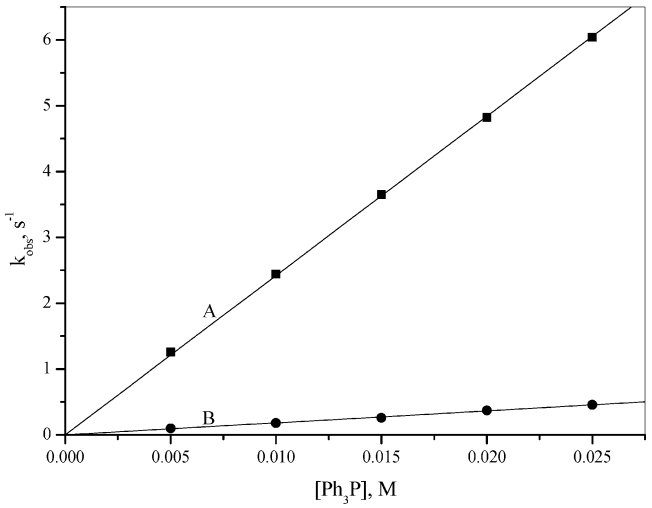


**Figure 3.** Plots of $k_{obs}$ versus [$Ph_3P$] for the reaction with $(0.5-1) \times 10^{-4}$ M *trans*-[Co(Hdmg)$_2$(R)MeOH] where R = $PhCH_2$ (A) and $CH_3$ (B) at 25.0 °C.

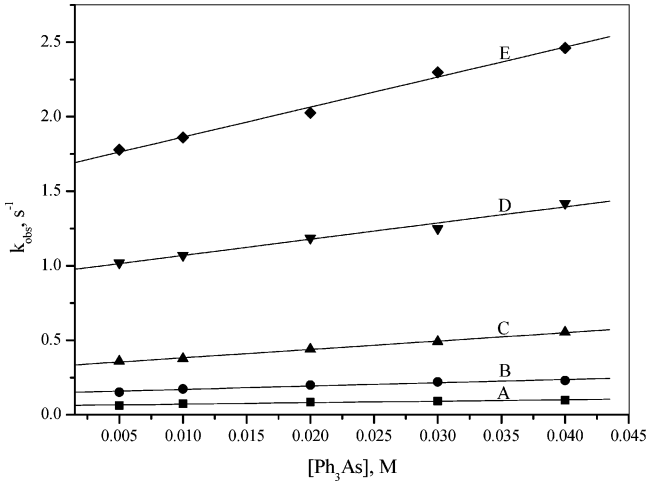


**Figure 4.** Plots of $k_{obs}$ versus [$Ph_3As$] for the reaction with *trans*-[Co(Hdmg)$_2$(Me)MeOH] as function of temperature. Experimental conditions: [$Co^{III}$] = $1 \times 10^{-4}$ M and $T = 5.0$ (A), 10.0 (B), 15.0 (C), 20.0 (D), and 25.0 (E) °C.

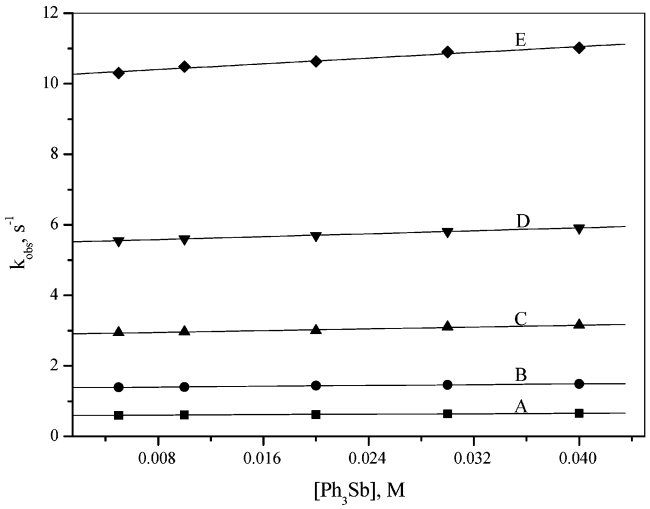


**Figure 5.** Plots of $k_{obs}$ versus [$Ph_3Sb$] for the reaction with *trans*-[Co(Hdmg)$_2$(Me)MeOH] as function of temperature. Experimental conditions: [$Co^{III}$] = $1 \times 10^{-4}$ M and $T = 5.0$ (A), 10.0 (B), 15.0 (C), 20.0 (D), and 25.0 (E) °C.

for the forward and reverse reactions in eq 1, respectively. Direct evidence for a reversible complex-formation reaction was obtained from the overall spectral changes observed during the reaction, which increased significantly with increasing entering nucleophile concentration. Unfortunately, the solubility of both $Ph_3As$ and $Ph_3Sb$ in methanol is too low to enable a direct spectrophotometric determination of the overall equilibrium constant. In the most favorable case, the ratio of $k_a/k_b$ (=12 $M^{-1}$ at 25 °C, see Table 3) in the case of $Ph_3As$ as entering ligand is such that a 1 M solution of the ligand will be required to shift the equilibrium over to the product side, whereas the solubility is limited to only 0.08 M at 25 °C.

Tables 3 and S1−S3 (Supporting Information) summarize the kinetic data obtained as a function of temperature and pressure for the series of reactions investigated. In the case of $Ph_3As$ and $Ph_3Sb$ as entering nucleophiles, the temperature and pressure dependence was studied at low and high nucleophile concentrations in order to determine the effect on $k_a$ and $k_b$, respectively. The values of $k_a$ and $k_b$ as a function of temperature and pressure, along with the corresponding activation parameters, are summarized in Table S3 (Supporting Information). Plots of ln $k_a$ and ln $k_b$ versus pressure gave good linear relationships as shown in Figure S2 (Supporting Information) for the reaction of *trans*-[Co(Hdmg)$_2$(R)MeOH] with $Ph_3As$, and the constructed volume profile is shown in Figure 6. Plots of ln $k_a$ versus pressure gave good linear relationships as shown in Figure S3 for the reaction of *trans*-[Co(Hdmg)$_2$(R)$H_2O$] with imidazole, pyrazole, 1,2,4-triazole, *N*-acetylimidazole, 5-chloro-1-methylimidazole, and $NO_2^-$. Similar plots are presented in Figure S4 (Supporting Information) for the reactions between *trans*-[Co(Hdmg)$_2$(R)MeOH] and $Ph_3P$ where (R = $CH_3$ and $PhCH_2$).

Second-order rate constants ($k_a$) for substitution of *trans*-[Co(Hdmg)$_2$(R)S] by the series of entering ligands in Table 3 at 25 °C do not depend strongly on the nature of the entering ligand either in aqueous or in methanol solution. The data in Table 4 show a similar trend except for

**Table 3.** Kinetic Data for the Reaction of *trans*-[Co(Hdmg)$_2$(R)S], for R = $CH_3$ and $PhCH_2$, and S = $H_2O$ and MeOH, with Different Nucleophiles (L)

| L[a] | $k_a$ at 25 °C, $M^{-1}\,s^{-1}$ | $\Delta H^{\ddagger}$, kJ $mol^{-1}$ | $\Delta S^{\ddagger}$, J $mol^{-1}\,K^{-1}$ | $\Delta V^{\ddagger}$, $cm^3\,mol^{-1}$ |
|---|---|---|---|---|
| imidazole[b,c] | 70.3 ± 0.5 | 74 ± 2 | +40 ± 8 | +3.7 ± 0.2 |
| pyrazole[b,c] | 91 ± 2 | 79 ± 2 | +56 ± 7 | +4.5 ± 0.4 |
| 1,2,4-triazole[b,c] | 70.6 ± 0.7 | 72 ± 3 | +31 ± 9 | +4.0 ± 0.1 |
| *N*-acetylimidazole[b,c] | 48 ± 1 | 70 ± 1 | +22 ± 3 | +3.1 ± 0.2 |
| 5-chloro-1-methylimidazole[b,c] | 105.1 ± 0.5 | 89 ± 2 | +92 ± 6 | +2.5 ± 0.1 |
| $NO_2^-$[b,c] | 113.9 ± 0.8 | 84 ± 3 | +78 ± 10 | +2.3 ± 0.1 |
| $Ph_3P$[d,e] | 19.6 ± 0.1 | 94 ± 2 | +97 ± 8 | +12.3 ± 0.4 |
| imidazole[d,e] | 23.6 ± 0.2 | 74 ± 2 | +29 ± 5 | +7.3 ± 0.1 |
| $Ph_3As_{(forward\ reaction)}$[d,e] | 20.1 ± 1.1 | 103 ± 4 | +126 ± 14 | +10.6 ± 0.5 |
| $Ph_3As_{(reverse\ reaction)}$[d,e] | 1.66 ± 0.03 $s^{-1}$ | 114 ± 5 | +143 ± 18 | +15.9 ± 0.2 |
| $Ph_3Sb_{(forward\ reaction)}$[d,e] | 20.3 ± 1.7 | 89 ± 3 | +77 ± 10 | |
| $Ph_3Sb_{(reverse\ reaction)}$[d,e] | 10.24 ± 0.04 $s^{-1}$ | 95 ± 3 | +95 ± 9 | +11.3 ± 0.4 |
| $Ph_3P$[f,g] | 252.0 ± 0.8 | 92 ± 1 | +109 ± 3 | +15.2 ± 0.3 |

[a] The two superscripts (b−e) given in the first column of the table refer to the experimental conditions selected for the temperature and pressure dependence studies, respectively (see Supporting Information). [b] *trans*-[Co(Hdmg)$_2$(Me)$H_2O$] = $1 \times 10^{-4}$ M, imidazole, pyrazole, 1,2,4-triazole, and *N*-acetylimidazole = 0.01−0.5 M, 5-chloro-1-methylimidazole = $1.88 \times 10^{-2}$ to 0.3 M, and $NO_2^-$ = $6.25 \times 10^{-2}$ to 0.5 M, pH 9.0, and $I$ = 0.1 M $NaClO_4$ and 0.5 M for $NO_2^-$ as ligand. [c] *trans*-[Co(Hdmg)$_2$(Me)$H_2O$] = $2 \times 10^{-4}$ M, imidazole, pyrazole, 1,2,4-triazole, and *N*-acetylimidazole = 0.01 M, 5-chloro-1-methylimidazole = $3.75 \times 10^{-2}$ M, and $NO_2^-$ = $6.25 \times 10^{-2}$ M, $T$ = 25.0 °C, pH 9.0, and $I$ = 0.1 M $NaClO_4$ and 0.5 M for $NO_2^-$ as ligand. [d] *trans*-[Co(Hdmg)$_2$(Me)MeOH] = $1 \times 10^{-4}$ M, [imidazole] = 0.05−0.5 M, [$Ph_3P$] = (0.5−2.5) $\times 10^{-2}$ M, [$Ph_3As$] and [$Ph_3Sb$] = (0.5−4.0) $\times 10^{-2}$ M. [e] *trans*-[Co(Hdmg)$_2$(Me)MeOH] = $2 \times 10^{-4}$ M, [imidazole] = 0.05 M, [$Ph_3P$] = 0.01 M, [$Ph_3As$] = (0.5−4.0) $\times 10^{-2}$ M, $T$ = 25.0 °C, and [$Ph_3Sb$] = 0.02 M at 15.0 °C. [f] *trans*-[Co(Hdmg)$_2$($PhCH_2$)MeOH] = $5 \times 10^{-5}$ M and [$Ph_3P$] = (0.5−2.5) $\times 10^{-2}$ M. [g] *trans*-[Co(Hdmg)$_2$($PhCH_2$)MeOH] = $5 \times 10^{-5}$ M and [$Ph_3P$] = 0.01 M at 25.0 °C.

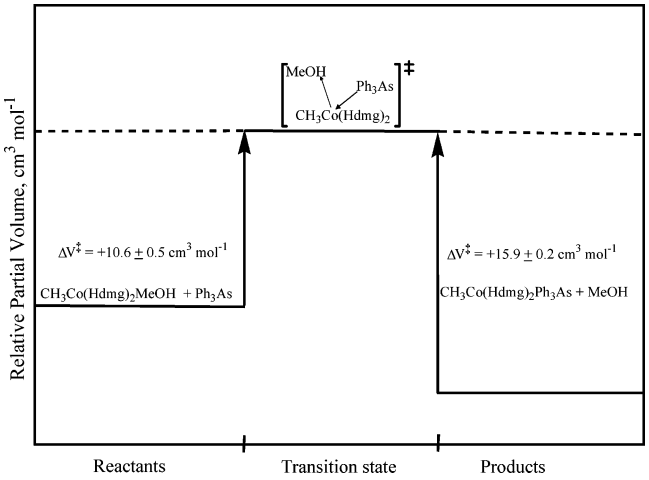


**Figure 6.** Volume profile for the following reaction:

*trans*-[Co(Hdmg)$_2$(R)MeOH] + $Ph_3As \underset{k_b}{\overset{k_a}{\rightleftharpoons}}$ *trans*-[Co(Hdmg)$_2$(R)As$Ph_3$] + MeOH

*N*-acetylimidazole as entering ligand (see further in Discussion). This is typical for a process that is dissociatively activated, either via a dissociative interchange ($I_d$) or limiting dissociative (D) mechanism, in which bond breakage with the leaving group largely controls the rate and nature of the substitution mechanism. Similarly, the rate constants for the backward reaction were found to be 1.7 and 10.2 $s^{-1}$ at 25 °C for the displacement of $Ph_3As$ and $Ph_3Sb$, respectively, indicating that the release of the nucleophile does depend on its nucleophilicity, again in line with a dissociatively activated mechanism controlled by bond cleavage with the leaving group. The most important factors that account for the increase in $k_b$ from $Ph_3P$ to $Ph_3As$ and $Ph_3Sb$ are the basicity and $\pi$-acceptor ability of these nucleophiles that decrease in this order. A more detailed discussion of the activation parameters given below reveals that a dissociative interchange mechanism ($I_d$) is favored, in terms of which the overall second-order rate constant $k_a$ is a composite of a precursor formation constant ($K$) and an interchange rate constant ($k$). This will further account for some of the differences in the values of $k_a$ especially in cases where precursor formation is favored by the nature of the entering nucleophile and so affects the value of $k_a$.

Substitution reactions of *trans*-[Co(Hdmg)$_2$(R)S] show a strong dependence on the nature of the alkyl group. The second-order rate constant for substitution of S = methanol by $Ph_3P$ was found to be 19.6 and 252 $M^{-1}\,s^{-1}$ at 25 °C for R = $CH_3$ and $PhCH_2$, respectively, and that for substitution of water by imidazole was found to be 70.3 and 20.9 $M^{-1}\,s^{-1}$ at 25 °C for R = $CH_3$ and $CH_2Cl$,[24] respectively. The lability of these complexes is affected by the size and electronic structure of the alkyl group. The second-order rate constant for substitution of *trans*-[Co(Hdmg)$_2$(R)$H_2O$] by pyrazole, 1,2,4-triazole, and *N*-acetylimidazole was found to be 1309, 1200, and 135 $M^{-1}\,s^{-1}$ for R = Et, 755, 691, and 119 $M^{-1}\,s^{-1}$ for R = $PhCH_2$, and 0.36, 0.35, and 0.07 $M^{-1}\,s^{-1}$ for R = $CF_3CH_2$ at 25 °C, respectively, as summarized in Table 4.[25] The second-order rate constants show that the kinetic *trans* effect decreases in the order Et > $PhCH_2$ > $CH_3$ > $CH_2Cl$ > $CF_3CH_2$ according to the donor properties of the alkyl group.

The solvent has a significant effect on the rate constant of the ligand substitution reaction. The second-order rate constant for substitution of the solvent in *trans*-[Co(Hdmg)$_2$(R)S] by imidazole was found be 70.3 and 23.6 $M^{-1}\,s^{-1}$ at 25 °C for S = $H_2O$ and MeOH, respectively. The slower reaction in methanol is ascribed to solvent effects and the fact that we are dealing with a totally different leaving group. The values of the second rate constant $k_a$ in MeOH are again independent of the nature of the entering nucleophile.

(24) Dreos-Garlatti, R.; Tauzher, G.; Costa, G. *Inorg. Chim. Acta* **1983**, *70*, 83.
(25) Hamza, M. S. A.; Felluga, A.; Randaccio, L.; Tauzher, G.; van Eldik, R. In preparation.

**Table 4.** Comparison of Rate and Activation Parameters for the Reaction of *trans*-[Co(chel)$_2$(R)H$_2$O] and Aquacobalamin with Imidazole, Pyrazole, 1,2,4-Triazole, and *N*-Acetylimidazole as Entering Nucleophiles

| ligand | $\Delta H^{\ddagger}$, kJ mol$^{-1}$ | $\Delta S^{\ddagger}$, J K$^{-1}$ mol$^{-1}$ | $\Delta V^{\ddagger}$, cm$^3$ mol$^{-1}$ | $k_a$, M$^{-1}$ s$^{-1}$ |
|---|---|---|---|---|
| | | *trans*-[Co(Hdmg)$_2$(Me)H$_2$O][a] | | |
| imidazole | 74 ± 2 | +40 ± 8 | +3.7 ± 0.2 | 70.3 ± 0.5 |
| pyrazole | 79 ± 2 | +56 ± 7 | +4.5 ± 0.4 | 90.7 ± 2.0 |
| 1,2,4-triazole | 72 ± 3 | +31 ± 9 | +4.0 ± 0.1 | 70.6 ± 0.7 |
| *N*-acetylimidazole | 70 ± 1 | +22 ± 3 | +3.1 ± 0.2 | 48.2 ± 1.0 |
| | | *trans*-[Co(Hdmg)$_2$(CH$_3$CH$_2$)H$_2$O][25,a] | | |
| pyrazole | 69 ± 0.6 | +46 ± 2 | +4.6 ± 0.3 | 1309 ± 14 |
| 1,2,4-triazole | 65 ± 1 | +31 ± 3 | +4.9 ± 0.3 | 1200 ± 7 |
| *N*-acetylimidazole | 72 ± 0.6 | +36 ± 2 | +4.1 ± 0.3 | 135 ± 2 |
| | | *trans*-[Co(Hdmg)$_2$(PhCH$_2$)H$_2$O][25,a] | | |
| pyrazole | 70 ± 2 | +46 ± 8 | +6.2 ± 0.5 | 755 ± 16 |
| 1,2,4-triazole | 66 ± 1 | +31 ± 3 | +7.5 ± 0.4 | 691 ±13 |
| *N*-acetylimidazole | 72 ± 1 | +38 ± 5 | +4.3 ± 0.3 | 119 ± 4 |
| | | *trans*-[Co(Hdmg)$_2$(CF$_3$CH$_2$)H$_2$O][25,a] | | |
| pyrazole | 83 ± 1 | +23 ± 3 | +4.4 ± 0.3 | 0.358 ± 0.006 |
| 1,2,4-triazole | 86 ± 2 | +37 ± 6 | +2.3 ± 0.3 | 0.348 ± 0.002 |
| *N*-acetylimidazole | 87 ± 2 | +26 ± 5 | +3.4 ± 0.3 | 0.069 ± 0.001 |
| | | *trans*-[Co(en)$_2$(Me)H$_2$O]$^{2+}$ [1,29] | | |
| imidazole[a] | 53 ± 2 | −22 ± 7 | +4.7 ± 0.1 | 198 ± 13 |
| pyrazole[b] | 67 ± 6 | +27 ± 19 | | 284 ± 10 |
| 1,2,4-triazole[b] | 59 ± 2 | +1 ± 6 | | 318 ± 5 |
| *N*-acetylimidazole[b] | 72 ± 4 | +23 ± 14 | | 24 ± 3 |
| | | aquacobalamin[12,30a] | | |
| imidazole | | | | 21.2 ± 0.7 |
| pyrazole | 85 ± 4 | +69 ± 13 | | 35.0 ± 0.8 |
| 1,2,4-triazole | 90 ± 2 | +83 ± 6 | | 24.0 ± 0.4 |
| *N*-acetylimidazole | 108 ± 12 | +135 ± 40 | +7.2 ± 0.3 | 6.6 ± 1.6 |

[a] The second rate constants were determined at 25.0 °C. [b] The second-order rate constants were calculated from the activation parameters for 25.0 °C.

The lability of organo cobaloximes is much higher than that of inorganic cobaloximes due to the alkyl group in the axial position that significantly increases the length of the Co−OH$_2$ bond in the ground state and increases its p$K_a$ value. p$K_a$ values were found to be 10.96[26] and 12.68[27] for *trans*-[Co(Hdmg)$_2$(CF$_3$CH$_2$)H$_2$O] and *trans*-[Co(Hdmg)$_2$(Me)H$_2$O], respectively. The activation enthalpy values for substitution of *trans*-[Co(Hdmg)$_2$(R)H$_2$O] by pyrazole, 1,2,4-triazole, and *N*-acetylimidazole for R = PhCH$_2$, CH$_3$, and CF$_3$CH$_2$ were found to be in the ranges 66−72,[25] 72−79, and 83−86 kJ mol$^{-1}$,[25] respectively, as summarized in Table 4. The activation entropies in Table 3 are in general significantly positive and in line with a dissociatively activated reaction mechanism. A plot of $\Delta H^{\ddagger}$ versus $\Delta S^{\ddagger}$ gives a good linear relationship for the reaction of *trans*-[Co(Hdmg)$_2$(Me)S] with imidazole, pyrazole, 1,2,4-triazole, *N*-acetylimidazole, 5-chloro-1-methylimidazole, and $NO_2^-$ in water as shown in Figure 7, and for the reaction with imidazole, Ph$_3$P, Ph$_3$As, and Ph$_3$Sb in MeOH as shown in Figure S5 (Supporting Information). The good compensation correlation between $\Delta H^{\ddagger}$ and $\Delta S^{\ddagger}$ suggests that an isokinetic relationship exists, which supports the claim that a single mechanism operates for the series of nucleophiles.[28]

The activation volumes for substitution of coordinated water in *trans*-[Co(Hdmg)$_2$(Me)H$_2$O] by imidazole, pyrazole, 1,2,4-triazole, *N*-acetylimidazole, 5-chloro-1-methylimidazole, and $NO_2^-$ were found to be between +2.3 and +4.5 cm$^3$ mol$^{-1}$. The relatively small positive values suggest that the reaction follows an I$_d$ mechanism in which the entering nucleophile is weakly bound in the transition state. The substitution of coordinated water by py and 4-CNpy in *trans*-[Co(Hdmg)$_2$(CF$_3$CH$_2$)H$_2$O] proceeds according to the same mechanism since $\Delta V^{\ddagger}$ was found to be +5.7 and +7.4 cm$^3$ mol$^{-1}$, respectively.[6] Similarly, $\Delta V^{\ddagger}$ values between +3.6 and +9.7 cm$^3$ mol$^{-1}$ were reported for displacement of water in *trans*-[Co(en)$_2$(Me)H$_2$O]$^{2+}$ [2,29] and in aquacobalamin[14,30]

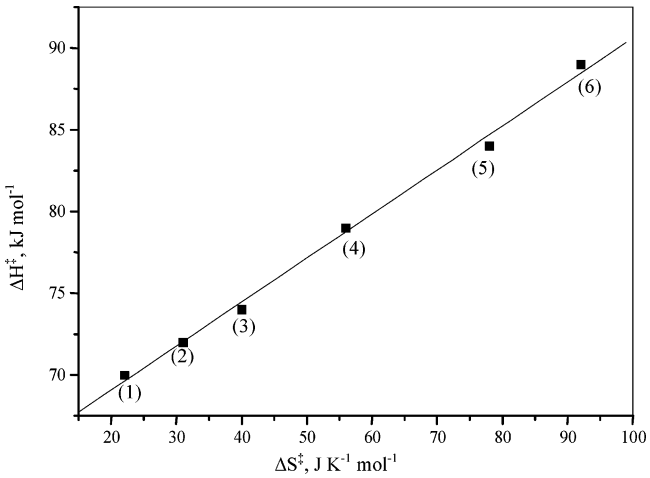


**Figure 7.** Correlation between $\Delta H^{\ddagger}$ and $\Delta S^{\ddagger}$ for the second-order rate constant for substitution of H$_2$O in *trans*-[Co(Hdmg)$_2$(Me)H$_2$O] by *N*-acetylimidazole (1), 1,2,4-triazole (2), imidazole (3), pyrazole (4), $NO_2^-$ (5), and 5-chloro-1-methylimidaziole (6).

(26) Brown, K. L.; Lyles, D.; Pencovici, M.; Kallen, R. G. *J. Am. Chem. Soc.* **1975**, *97*, 7338.
(27) Brown, K. L.; Chernoff, D.; Keljo, D. J.; Kallen, R. G. *J. Am. Chem. Soc.* **1972**, *94*, 6697.
(28) Espenson, J. H. *Chemical Kinetics and Reaction Mechanisms*; McGraw-Hill: New York, 1995, p 164.
(29) Hamza, M. S. A. *J. Coord. Chem.* **2003**, *56*, 553.

by different nucleophiles. $\Delta V^{\ddagger}$ values for the substitution of water by *N*-acetylimidazole in *trans*-$[Co(Hdmg)_2(Me)H_2O]$ and aquacobalamin[12] were found to be +3.1 and +7.2 $cm^3$ $mol^{-1}$, respectively. Similar data for ligand substitution reactions of *trans*-$[Co(Hdmg)_2(R)H_2O]$ by 1,2,4-triazole for R = $CF_3CH_2$,[25] $CH_3$, and $PhCH_2$[25] were found to be +2.3, +3.2, and +7.5 $cm^3$ $mol^{-1}$, respectively, as summarized in Table 4. These values all favor a dissociative interchange mechanism that consists of rapid precursor formation and a rate-determining interchange reaction. The consequence is that the overall second-order rate constant $k_a$ is a composite value of the precursor formation constant ($K$) and the interchange rate constant ($k$), such that $k_a = kK$ as mentioned above. This naturally complicates the interpretation of $k_a$ and its activation parameters since it was not possible to separate $k$ and $K$ (and their thermodynamic parameters) kinetically in the studied reactions, as could be done in other cases.[6,13]

As mentioned before, activation volumes for ligand substitution reactions on $[Co(TMPP)(H_2O)_2]^{5+}$ and $[Co(TPPS)(H_2O)_2]^{3-}$ (TMPP = *meso*-tetrakis(4-*N*-methylpyridyl)porphine and TPPS = *meso*-tetrakis(*p*-sulfonatophenyl)porphine) are +14.4 and +15.4 $cm^3$ $mol^{-1}$, respectively,[16,17] and were assigned to a limiting D mechanism. The activation volumes for the substitution of methanol in *trans*-$[Co(Hdmg)_2(R)MeOH]$ by $Ph_3P$ for R = $CH_3$ and $PhCH_2$ were also found to be more positive, viz. +12.3 and +15.2 $cm^3$ $mol^{-1}$, respectively, which could suggest the operation of a limiting dissociative mechanism. However, this trend could also be due to the larger partial molar volume of methanol as compared to water, since this will affect the magnitude of $\Delta V^{\ddagger}$ for a dissociatively activated process. By way of comparison, it is interesting to note that the reaction of *trans*-$[Co(Hdmg)_2(CH_3)MeOH]$ with imidazole is characterized by a significantly smaller activation volume than that found for $Ph_3P$, which suggests the operation of a dissociative interchange mechanism. The reason for this apparent difference in mechanism may be related to the formation of a precursor complex with imidazole, which would then favor a dissociative interchange mechanism in which precursor formation will contribute to the overall activation parameters found for $k_a$ since $k_a = kK$.

In one system, it was possible to construct a volume profile for the reaction between *trans*-$[Co(Hdmg)_2(Me)MeOH]$ and $Ph_3As$ (Figure 6), from which the dissociative character of the substitution process is clearly seen. The larger $\Delta V^{\ddagger}$ for the back reaction is related to the larger partial molar volume of the leaving ligand $Ph_3As$, which also accounts for the overall negative reaction volume. Although these larger activation volumes tend to suggest the operation of a limiting D mechanism, this suggestion is speculative due to the uncertain contribution of the larger partial molar volumes of the leaving groups for both the forward and back reactions as outlined above. In the case of a dissociative interchange $I_d$ mechanism, the volume of activation for the forward reaction will include contributions arising from precursor formation and the interchange reaction step since $k_a = kK$ and $\Delta V^{\ddagger}(k_a) = \Delta V^{\ddagger}(k) + \Delta V(K)$. Due to our inability to separate $k$ and $K$ kinetically in the present case, no further details can be included in the volume profile.

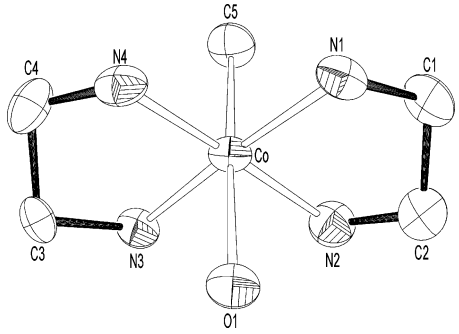


**Figure 8.** Crystal structure of the cation *trans*-$[Co(en)_2(Me)H_2O]^{2+}$.

**Table 5.** Structural Parameters for Complexes of the Type *trans*-$[Co(chel)_2(X)H_2O]$, Where chel Represents the Equatorial Chelate Ligand

| X | Co−O (Å) | Co−X(Å) | O−Co−X (deg) |
|---|---|---|---|
| | *trans*-$[Co(en)_2(X)H_2O]^{2+}$ | | |
| $CH_3$ | 2.153(6) | 1.995(10) | 177.6(3) |
| | *trans*-$[Co((DO)(DOH)pn)(X)H_2O]^{+}$ | | |
| $CH_3$[34] | 2.14(2) | 1.99(4) | |
| | *trans*-$[Co((EMO)(EMOH)pn)(X)H_2O]^{+}$ | | |
| $CH_3$[31] | 2.102(3) | 1.997(4) | |
| | *trans*-$[Co(Hdmg)_2(X)H_2O]$ | | |
| $CH_3$[33] | 2.058(3) | 1.990(5) | 178.0(2) |
| $CH_2CMe_3$[32] | 2.056(5) | 2.044(7) | 172.4(3) |
| $CN$[32] | 1.992(4) | 1.906(5) | |
| $NO_2$[32] | 1.980(5) | 1.881(9) | |
| $Br$[32] | 1.955(11) | 2.364(2) | 180.0 |

The labilization of the ligand in the position *trans* to the cobalt−carbon bond can in many cases be observed in the ground state as a result of the *trans* influence. In the present study, it was possible to crystallize *trans*-$[Co(en)_2(Me)H_2O]$-$S_2O_6$ of which the structure, determined by X-ray analysis, is shown in Figure 8. The crystal consists of organometallic cations and dithionate anions. The structure of the complex is a distorted octahedron, the cobalt atom and the four nitrogen atoms are located in the equatorial plane, and the water molecule and methyl group occupy the axial positions as shown in Figure 8. The Co−O and Co−C bond lengths in *trans*-$[Co(en)_2(Me)H_2O]^{2+}$ were found to be 2.153(6) and 1.995(10) Å, respectively, and the Co−N bond lengths for N(1), N(2), N(3), and N(4) were found to be 1.999(7), 1.995(8), 1.931(7), and 1.927(7) Å, respectively. The significantly larger Co−N(1) and Co−N(2) distances can be ascribed to the influence of hydrogen bonding to the oxygen atoms of the $S_2O_6^{2-}$ anion, which is located close to these amines in the crystal structure.

A comparison of the crystal structure data with closely related complexes is given in Table 5. The bond lengths depend on the nature of alkyl group and the equatorial ligands, the hybridization state of the carbon bond attached to the cobalt center, and steric interactions between the axial alkyl and the equatorial ligands (steric *cis* influence).[31,32] In addition, the overall charge on the complexes changes from

(30) Marques, H. M.; Egan, T. J.; Marsh, J. H.; Mellor, J. R.; Munro, O. Q. *Inorg. Chim. Acta* **1989**, *166*, 249.

(31) Marzilli, L. G.; Bresciani-Pahor, N.; Randacio, L.; Zangrando, E.; Finke, R. G.; Myers, S. A. *Inorg. Chim. Acta* **1985**, *107*, 139.

2+ to zero, which will also affect the metal−ligand bond lengths and complicate the following comparison. The X-ray structure data show that the bond lengths of Co−O are 2.058(3),[33] 2.102(3),[31] 2.14(2),[34] and 2.153(6) Å for *trans*-[Co(Hdmg)$_2$(Me)H$_2$O], *trans*-[Co((EMO)(EMOH)pn)(Me)H$_2$O]$^+$, *trans*-[Co((DO)(DOH)pn)(Me)H$_2$O]$^+$, and *trans*-[Co(en)$_2$(Me)H$_2$O]$^{2+}$, respectively, where (DO)(DOH)pn = diacetylmonoxime-diacetyl monoximato-propane-1,3-diyldiimino and (EMO)(EMOH)pn = 3,9-dimethyl-2,10-diethyl-1,4,8,11-tetraazaundeca-1,3,8,10-tetraen-11-ol-1-olato. These data show that the Co−OH$_2$ bond is stronger in the ground state in the case of *trans*-[Co(Hdmg)$_2$(Me)H$_2$O]. The Co−O bond length increases from 1.955(4) Å for X = Br to 2.058(3) Å for X = CH$_3$ in the complex *trans*-[Co(Hdmg)$_2$(X)H$_2$O] as shown in the Table 5.[32] A comparison of the data in Table 5 indicates that several kinds of structural changes arise from changes in the electron-donating ability of R and from the interactions between the alkyl group and the equatorial moiety, and the nature of the equatorial ligand. The Co−C bond lengthens from 1.990 to 2.044 Å as the bulk of the alkyl group increases from CH$_3$ to CH$_2$CMe$_3$ in the case of the dimethylglyoximate complex, and clearly depends on the steric interaction between the axial alkyl and the equatorial ligands.[31] In addition, the hybridization of the carbon atom affects the Co−C bond length, which was found to be 2.00, 1.96, and 1.90 Å for sp$^3$, sp$^2$, and sp hybridization, respectively.[32] Distortion arising from the interaction of the axial alkyl group with the equatorial ligand can be ascribed to (a) changes in the C−Co−N(eq) bond angles; (b) widening of the Co−CH$_2$−R′ angles and shortening of the Co−R bond lengths; (c) lengthening of the Co−C bond; (d) deformation of the equatorial ligand unit.[32]

It can be concluded that the variety of chelates, R groups, entering ligands, and solvents selected in this and our earlier studies[1−6] enables a systematic tuning of the lability of alkyl cobalt(III) complexes, which results in a systematic tuning of the ligand displacement process in terms of a dissociative interchange (I$_d$) and a limiting dissociative (D) mechanism.

**Acknowledgment.** The authors gratefully acknowledge financial support from the Deutsche Forschungsgemeinschaft (SFB 583 "Redox-active metal complexes"), Fonds der Chemischen Industrie, and the Max-Buchner Forschungsstiftung. We thank Alessandro Felluga, Lucio Randaccio, and Giovanni Tauzher, Università degli Studi di Trieste, Italy, for providing samples of the complexes used in this study.

**Supporting Information Available:** Crystallographic data in CIF format. Additional tables and figures. This material is available free of charge via the Internet at http://pubs.acs.org.

IC049761J

(32) Bresciani-Pahor, N.; Forcolin, M.; Marzilli, L. G.; Randaccio, L. Summers, M. F.; Toscano, P. J. *Coord. Chem. Rev.* **1985**, *63*, 1.
(33) McFadden, D. L.; McPhail, A. T. *J. Chem. Soc., Dalton Trans.* **1974**, 363.
(34) Bückner, S.; Calligaris, M.; Nardin, G.; Randaccio, L. *Inorg. Chim. Acta* **1969**, *3*, 278.